

Appendix

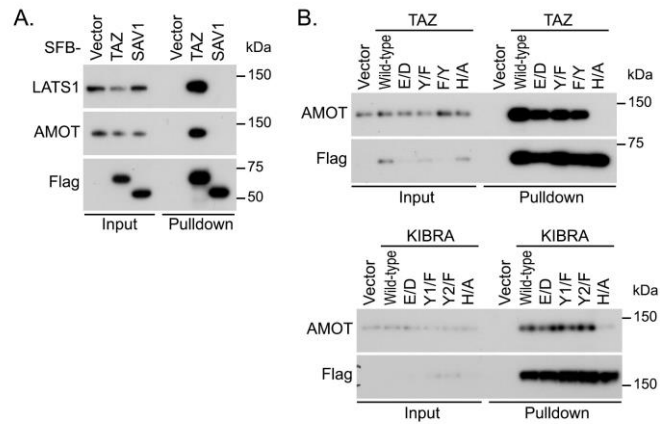
Elucidation of the Hippo WW domain determinants reveals STXBP4 as a Hippo pathway regulator

This Appendix file contains:

Appendix Figures S1-S8

Appendix Table S1

Appendix Figure S1



Appendix Figure S1. Characterization of the Hippo WW domain binding specificity. (This figure is related to Figure 2).

(A) Hippo pathway components TAZ but not SAV1 interacts with AMOT and LATS1.

HEK293T cells were transfected with the indicated SFB-tagged constructs and subjected to the pulldown assay.

(B) Examination of the conservative substitution mutations for the identified 9-amino acid sequence. HEK293T cells were transfected with the indicated SFB-tagged constructs and subjected to the pulldown assay. The tandem tyrosine residues within the 9-amino acid sequence of KIBRA were indicated as Y1 and Y2, respectively.

Appendix Figure S2

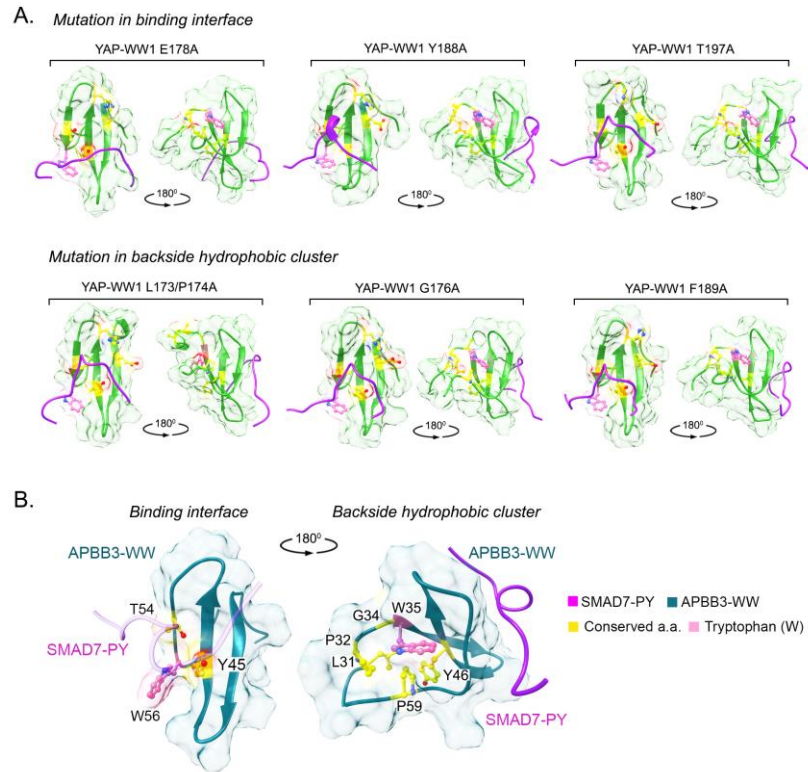
```

Yorkie-WW1 1 GALPPGWEQAKTND-GQIYYLNHTTKSTQWEDPRI 34
Yorkie-WW2 1 GPLPDGWEQAVTES-GDLYFINHIDRTTSWNDPRM 34
Salvador-WW 1 LPLPPGWATQYTLH-GRKYYIDHNAHTTHWNHPLE 34
Kibra-WW 1  FPLPDGWDIAKDFD-GKTYIDHINKKTTWLDPRD 34
--LP-GWE-----YY--H----T-W--P--
      (D)          (FF)

```

Appendix Figure S2. Examination of the identified 9-amino acid sequence for the *Drosophila* Hippo pathway components. (This figure is related to Figure 2 and Figure EV2).

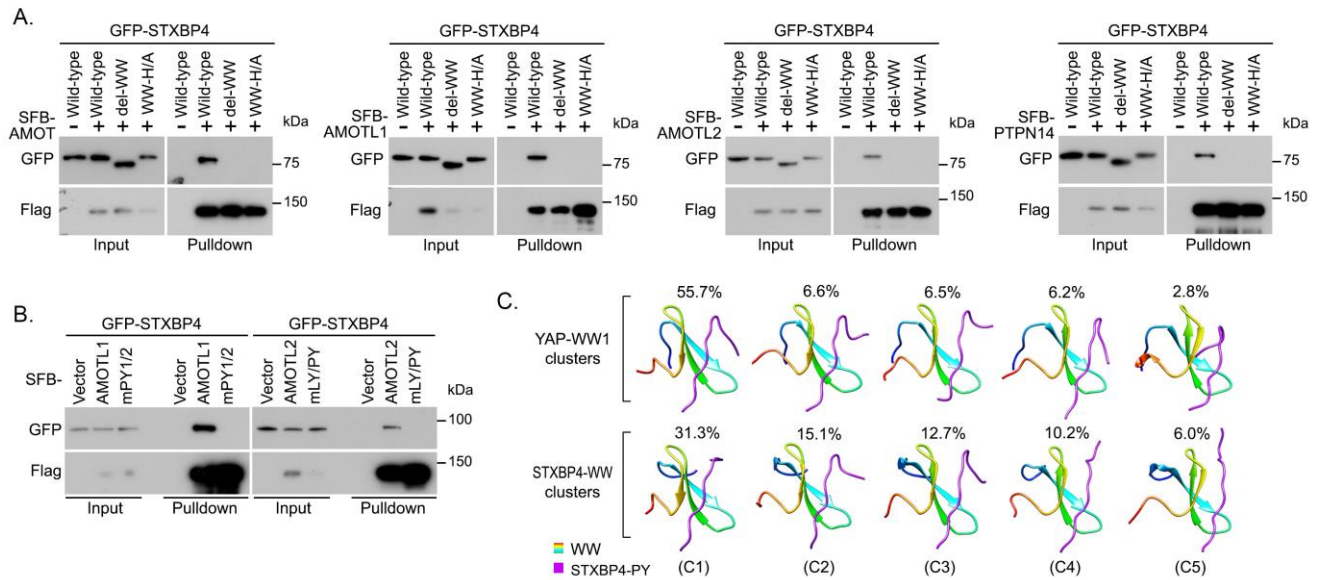
Sequence alignment of the WW domains derived from the *Drosophila* Hippo WW domain-containing components. The two conserved tryptophan residues were highlighted in purple. As compared with the 9-amino acid sequence, the conserved amino acid residues were highlighted in yellow.



Appendix Figure S3. Characterization of the identified 9-amino acid sequence through simulation analyses. (This figure is related to Figure EV3).

(A) Simulation analysis of the indicated YAP-WW1 mutant/SMAD7-PY complexes.

(B) Illustration of the identified 9-amino acid sequence in the APBB3-WW/SMAD7-PY complex. The NMR solution structure of the APBB3-WW domain (2YSC) was used for simulation. SMAD7-PY peptide was adjusted to 50% transparency to show the residue details on the binding interface.



Appendix Figure S4. STXB4 associates with the Hippo PY motif-containing proteins.

(This figure is related to Figure 3).

(A and B) The association between STXB4 and the indicated Hippo PY motif-containing proteins is mediated by the WW domain (A) and PY motif (B). HEK293T cells were transfected with the indicated constructs and subjected to the pulldown assay.

(C) Simulation of the STXB4-WW and SMAD7-PY complex structure. The top five WW-PY structure clusters were shown for both YAP-WW1/SMAD7-PY and STXB4-WW/SMAD7-PY complexes. The frequency rate was shown for each cluster. C, cluster.

Chromosome 17: 54,990,799–54,991,025 Exon 3 gRNA4 gRNA5 PAM

CTCTAGATCTCAGATTTTGATTTAATAAGTAGTTTTAAAGAAAAAATAGGTGCAGATCTCTAGACTAACCTGTG
TGTGCTAATTTACTTTATCTTAGGGATCCTGCCTTTCAGATGATTACAATTGCCAAGGAAACAGGCCTTGGCCT
GAAGGTAAGTAAATAATGTCCTATGCCACCAAAAATACAAAACAAAAGACCACCAGTGGTAAAGTTTATTT
TTCTCTCTTTATTAGTGAATTTATATCCACTGTGACCATACCTCAGT

STXBP4-KO1# 1bp deletion

CTCTAGATCTCAGATTTTGATTTAATAAGTAGTTTTAAAGAAAAAATAGGTGCAGATCTCTAGACTAACCTGTG
TGTGCTAATTTACTTTATCTTAGGGATCCTGCCTTTCAGATGATTACAATTG-CAAGGAAACAGGCCTTGGCCT
GAAGGTAAGTAAATAATGTCCTATGCCACCAAAAATACAAAACAAAAGACCACCAGTGGTAAAGTTTATTT
-----TAAGTAAATAATGTCCTATGCCACCAAAAATACAAAACAAAAGACCACCAGTGGTAAAGTTTATTT
TTCTCTCTTTATTAGTGAATTTATATCCACTGTGACCATACCTCAGT 58bp deletion

STXBP4-KO2#

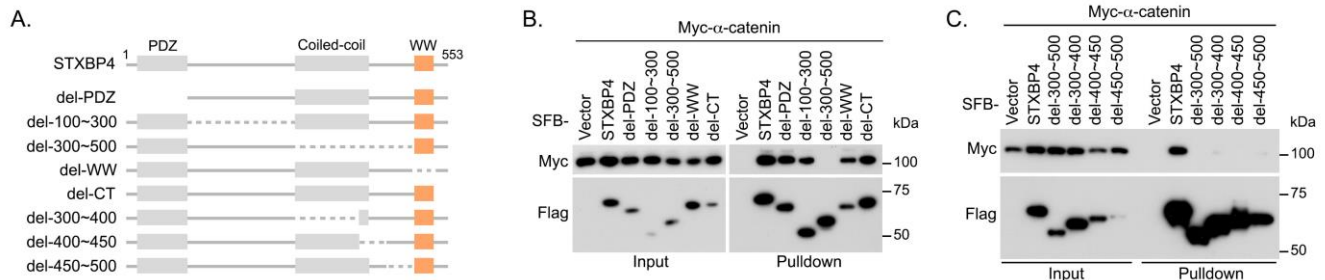
CTCTAGATCTCAGATTTTGATTTAATAAGTAGTTTTAAAGAAAAAATAGGTGCAGATCTCTAGACTAACCTGTG
TGTGCTAATTTACTTTATCTTAGGGATCCTGCCTTTCAGATGATTACAATTG-----TTGGCCT 41bp deletion
-----AACCAGGAATGAAGGCCCATTTGGTATATATTTCAGGAAATTTCTTGGAGGAGACT
GTTATAAGTAAATAATGTCCTATGCCACCAAAAATACAAAACAAAAGACCACCAGTGGTAAAGTTTATTT
TTCTCTCTTTATTAGTGAATTTATATCCACTGTGACCATACCTCAGT

STXBP4-KO3# 13bp deletion

CTCTAGATCTCAGATTTTGATTTAATAAGTAGTTTTAAAGAAAAAATAGGTGCAGATCTCTAGACTAACCTGTG
TGTGCTAATTTACTTTATCTTAGGGATCCTGCCTTTCAGATGATTACAATTGCC-----TTGGCCT
GAAGGTAAGTAAATAATGTCCTATGCCACCAAAAATACAAAACAAAAGACCACCAGTGGTAAAGTTTATTT
GTTATAAGTAAATAATGTCCTATGCCACCAAAAATACAAAACAAAAGACCACCAGTGGTAAAGTTTATTT
TTCTCTCTTTATTAGTGAATTTATATCCACTGTGACCATACCTCAGT

Appendix Figure S5. Genomic DNA sequencing results for the STXBP4 knockout (KO) cell lines as generated via CRISPR/Cas9. (This figure is related to Figure 3).

Among the five designed guide RNAs (gRNAs), only the gRNA4 and gRNA5-targeted regions showed genomic editing for all the three STXBP4 KO cell lines. The genomic editing details for each STXBP4 KO cell line were indicated.

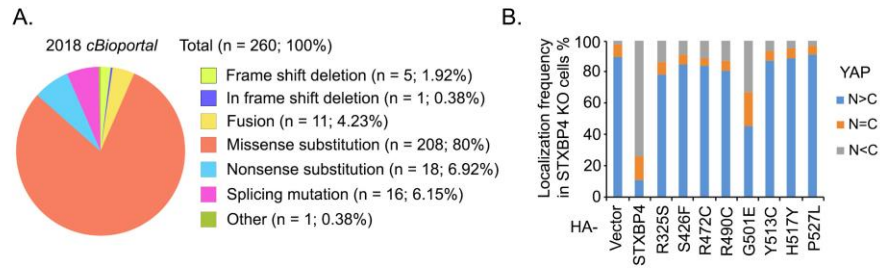


Appendix Figure S6. STXBP4 interacts with α -catenin. (This figure is related to Figure 4).

(A) Schematic illustration of a series of STXBP4 protein truncation and deletion mutants used in this study.

(B and C) Mapping the α -catenin binding region in STXBP4. An internal region (300~500 residues) of STXBP4 is required to associate with α -catenin (B), and we failed to further narrow down the binding region within the 300~500 residues (C).

Appendix Figure S7

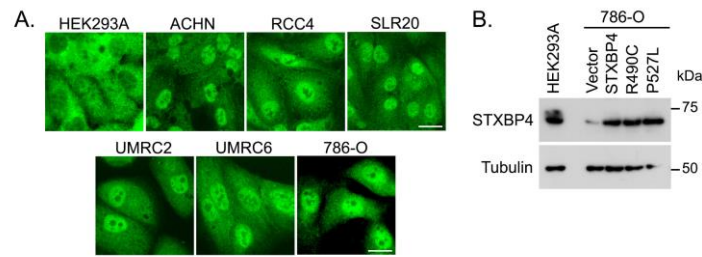


Appendix Figure S7. STXBP4 binds α -catenin and AMOT to regulate YAP. (This figure is related to Figure 4).

(A) Summary of STXBP4 mutations in cBioportal web database (<http://www.cbioportal.org>).

(B) Interactions with α -catenin and the Hippo PY motif-containing proteins are both required for the STXBP4-mediated YAP suppression. The indicated STXBP4 mutants were expressed in the STXBP4 KO cells and immunofluorescent staining was performed. HA-positive cells from ~30 different views (~200 cells in total) were randomly selected and quantified for YAP localization. N, nuclear localization. C, cytoplasmic localization.

Appendix Figure S8



Appendix Figure S8. STXBP4 is a potential tumor suppressor in kidney cancer. (This figure is related to Figure 5).

(A) YAP is highly enriched in the tested ccRCC cancer cell lines. YAP cellular localization is detected by immunofluorescent staining. Scale bar, 20 μ m.

(B) STXBP4 protein expression is examined in the 786-O cells that were transduced with STXBP4 and its cancer-derived mutants.

Appendix Table S1: Simulation Conditions

Structure	# of Simulations	PDB ID	Temperature (K)	Start – End Time per sim. (μs)	Ions & Waters
(WT) YAP- WW1 & SMAD7	3	2LTW	300	0.4–1	1 Na+ 3147waters
(WT) STXBP4-WW & SMAD7	3	2YSG, 2LTW	300	0.6–1	3 Na+ 4222waters
(WT) APBB3-WW & SMAD7	3	2YSC, 2LTW	300	0-1	1 Cl- 3897- 5433waters
(Mutant) YAP-WW1 <u>L173A/P174A</u> & SMAD7	3	2LTW	300	0-1	1 Na+ 3048- 4496waters
(Mutant) YAP-WW1 <u>G176A</u> & SMAD7	3	2LTW	300	0-1	1 Na+ 2880- 3528waters
(Mutant) YAP-WW1 <u>W177A</u> & SMAD7	3	2LTW	300	0-1	1 Na+ 3235- 4118waters
(Mutant) YAP-WW1 <u>E178A</u> & SMAD7	3	2LTW	300	0-1	3365- 3546waters
(Mutant) YAP-WW1 <u>Y188A</u> & SMAD7	3	2LTW	300	0-1	1 Na+ 3292- 4430waters
(Mutant) YAP-WW1 <u>F189A</u> & SMAD7	3	2LTW	300	0-1	1 Na+ 3260- 3831waters
(Mutant) YAP-WW1 <u>H192A</u> & SMAD7	3	2LTW	300	0-1	1 Na+ 2916- 4162waters
(Mutant) YAP-WW1 <u>T197A</u> & SMAD7	3	2LTW	300	0-1	1 Na+ 2872- 3139waters
(Mutant) YAP-WW1 <u>W199A</u> & SMAD7	3	2LTW	300	0-1	1 Na+ 3608- 3974waters
(Mutant) YAP-WW1 <u>P202A</u> & SMAD7	3	2LTW	300	0-1	1 Na+ 2789- 3887waters

(WT) apo YAP-WW1	3	2LTW	300	0-1	2870waters
(Mutant) apo YAP-WW1 <u>L173A/P174A</u>	3	2LTW	300	0-1	2669- 2739waters
(Mutant) apo YAP-WW1 <u>G176A</u>	3	2LTW	300	0-1	2761-2998 waters
(Mutant) apo YAP-WW1 <u>W177A</u>	3	2LTW	300	0-1	2839-2988 waters
(Mutant) apo YAP-WW1 <u>E178A</u>	3	2LTW	300	0-1	1Cl- 2813-3088 waters
(Mutant) apo YAP-WW1 <u>Y188A</u>	3	2LTW	300	0-1	2661- 3097waters
(Mutant) apo YAP-WW1 <u>F189A</u>	3	2LTW	300	0-1	2882-2996 waters
(Mutant) apo YAP-WW1 <u>H192A</u>	3	2LTW	300	0-1	2834-2974 waters
(Mutant) apo YAP-WW1 <u>T197A</u>	3	2LTW	300	0-1	2822-3022 waters
(Mutant) apo YAP-WW1 <u>W199A</u>	3	2LTW	300	0-1	2788-2934 waters
(Mutant) apo YAP-WW1 <u>P202A</u>	3	2LTW	300	0-1	2773-3008 waters

Appendix Table S1. List of simulation conditions. (This table is related to Figure 3, Figure EV3 and Appendix Figure S3).

Summary of all the structural simulation conditions and time/frames used for all the indicated analyses. The start and end times for the YAP-WW1 and STXBP4-WW complexes were determined via convergence analyses of MM/PBSA calculations.